SKB

TECHNICAL REPORT 89-27

Post-excavation analysis of a revised hydraulic model of the Room 209 fracture, URL, Manitoba, Canada
A part of the joint AECL/SKB characterization of the 240 m level at the URL, Manitoba, Canada

Anders Winberg[1], Tin Chan[2], Peter Griffiths[2], Blair Nakka[2]
[1] Swedish Geological Co, Gothenburg, Sweden
[2] Computations & Analysis Section, Applied Geoscience Branch, Atomic Energy of Canada Limited, Pinawa, Manitoba, Canada

October 1989

SVENSK KÄRNBRÄNSLEHANTERING AB
SWEDISH NUCLEAR FUEL AND WASTE MANAGEMENT CO
BOX 5864 S-102 48 STOCKHOLM
TEL 08-665 28 00 TELEX 13108 SKB

POST-EXCAVATION ANALYSIS OF A REVISED HYDRAULIC MODEL OF THE ROOM 209 FRACTURE, URL, MANITOBA, CANADA
A PART OF THE JOINT AECL/SKB CHARACTERIZATION OF THE 240 M LEVEL AT THE URL, MANITOBA, CANADA

Anders Winberg[1], Tin Chan[2], Peter Griffiths[2], Blair Nakka[2]

1 Swedish Geological Co, Gothenburg, Sweden
2 Computations & Analysis Section, Applied Geoscience Branch, Atomic Energy of Canada Limited, Pinawa, Manitoba, Canada

October 1989

SWEDISH GEOLOGICAL CO
Engineering Geology Division
Client : SKB

REPORT
Date : 1988-11-16
Revised : 1989-09-26
ID-no : IRAP 88420

POST-EXCAVATION ANALYSIS OF A REVISED HYDRAULIC MODEL OF THE ROOM 209 FRACTURE, URL, MANITOBA, CANADA

A part of the joint AECL/SKB characterization
of the 240 m level at the URL, Manitoba, Canada

by

Anders Winberg[1)]
Tin Chan[2)]
Peter Griffiths[2)]
Blair Nakka[2)]

[1)]Swedish Geological Co
Göteborg, Sweden

[2)]Computations & Analysis Section
Applied Geoscience Branch
Atomic Energy of Canada Limited
Pinawa, Manitoba, Canada

Abstract

An excavation response test was conducted in the Room 209 on the 240 m level of the AECL Underground Research Laboratory. Model predictions prior to excavation were made of the geo-mechanical response of the rock mass and the hydraulic response of an intercepted fracture. The model results were compared with excavation response data collected in a comprehensive instrument array.

The work performed has addressed discrepancies between calculated and in-situ measured hydraulic response as part of a post-test analysis. Already existing hydraulic conceptual models of the fracture were revised and any available information was included in the new model.

The model reproduced the pre-excavation hydraulic head distribution and hydraulic test results in terms of normalized flow rate within 5% and 75%, respectively. It was also found that the model reproduced the results of cross-hole hydraulic interference tests at least from a qualitative standpoint.

The next stage of the modelling addressed the response of the model to a simulation of the excavated pilot tunnel. The preliminary results suggested the presence of a skin of different permeability in a thin zone around the periphery of the tunnel. By altering the permeability in the floor and along the walls and roof of the periphery, a better correspondence between calculated and measured drawdown was obtained. The same also applied for measured groundwater inflow in quantity, though not for the actual distribution of inflow.

As probable causes for the interpreted positive skin in the crown and wall, temporary partial unsaturation and propulsion of debris into the fracture were suggested. The negative skin in the floor was interpreted as an effect of the dense and high energy charges used in the excavation process.

Executive summary

An excavation response test was conducted in the Room 209 at the 240 m level of the AECL Underground Research Laboratory. Prior to excavation, model predictions were made of the geomechanical response of the rock mass and the hydraulic response of an intercepted fracture. The model results were compared with excavation response data collected in a comprehensive instrument array.

The work reported here addresses the discrepancies between calculated and in-situ measured hydraulic response as part of a post-excavation analysis of the test. Existing hydraulic conceptual models of the fracture adopting the parallel plate approach were revised and any available information was included in the new model. A gradient in the fracture inferred from pressure readings in new boreholes was included in the revised model. In addition existing boreholes close to the tunnel periphery were included explicitly with a dense discretization to facilitate simulation of the hydraulic tests performed.

The model was calibrated by matching the model results in terms of pre-excavation steady state head distribution and the simulated single-hole hydraulic tests with the corresponding in-situ data. The model reproduced the head distribution within 5% and the test results in terms of normalized flow rate within 75%. It was also found that the model reproduced the results of cross-hole interference tests at least from a qualitative standpoint. It was concluded that with the assumptions made the model used may be considered as a reasonable representation of the in-situ pre-excavation conditions.

The next stage of the modelling addressed the response of the model to a simulation of the excavated pilot tunnel. It was found that the drawdown due to excavation at the points of the simulated boreholes in some cases were overestimated with up to a factor 30. Correspondingly the inflow to the tunnel was overestimated by an order of magnitude. With a few exceptions the simulated drawdown tests in the boreholes yielded an overestimation of the normalized flow rate by up to 40%.

The results suggested the presence of a skin of different permeability in a thin zone ($\approx$1 m) around the periphery of the tunnel. By increasing the permeability of this skin zone in the floor by an order of magnitude and decreasing the skin zone permeability in the walls and roof of the periphery by the same amount in relation to the least permeable unit of the model, a better correspondence between calculated and measured drawdown was obtained. The same also applied to measured groundwater inflow in quantity, though not for the actual distribution of inflow. The model with skin included was also found to better describe the relative change in normalized flow rate between the pre- and post-excavation conditions (introduction of pilot tunnel).

As probable causes for the positive skin (decreased permeability) in the crown and wall, temporary partial unsaturation and propulsion of debris into the fracture were suggested. The negative skin in the floor was interpreted as an effect of the dense and high energy charges used in the excavation process. The normal stiffness of the fracture is so high that possible changes in fracture hydraulics due to the small normal stress changes inferred are expected to be small.

In light of a possible Operating Phase migration and sorption experiment in the Room 209 fracture it was recommended to secure more far field data with regard to boundary conditions and material properties.

It was also recommended to conduct a similar experiment in parallel tunnels using careful explosive techniques and tunnel boring machines. This would facilitate means to better distinguish between effects of pure stress redistribution and that of the excavation.

CONTENTS

1. INTRODUCTION

One focus of geoscience research within the Canadian Nuclear Fuel Waste Management Program is the AECL Underground Research Laboratory (URL) near Pinawa, Manitoba. A unique feature of the URL is the fact that it is located in a previously undisturbed part of a large granitic pluton, the Lac du Bonnet batholith. The principal objectives of the URL Project are (Simmons 1988):

- to assess airborne, surface and subsurface survey techniques for characterization of the subsurface geological and hydrogeological environment in plutonic rock.

- to assess the changes in physical and chemical conditions in the rock mass and groundwater caused by excavation of the URL, and

- to perform experiments relevant to assessing the performance of the disposal system being considered in Canada (multibarrier system with a low solubility waste form, corrosion resistant container, low-permeable clay-based buffer and backfill, and finally a stable geosphere that separates the emplaced waste from the biosphere) for nuclear fuel waste disposal.

Prior to development, the site (3.8 km^2) of the facility was well characterized in a series of investigation stages which eventually led up to the development of geological and hydrogeological conceptual models of the area (Davison et al 1987). The final hydrogeological conceptual model was calibrated against large scale field tests and was tested by predicting the responses of the hydrogeological regime due to the excavation of the access shaft to 240 m depth.

The shaft and the subsequently excavated experiment level at the 240 m level have been subject to extensive geological characterization. In parallel the hydrogeological monitoring network has been extended with subsurface borehole installations. In addition an extensive geomechanical program has been carried out in the shaft and on the 240 m level to assess the spatial variation in in-situ stresses and the disturbance in the stress field around underground openings imposed by the excavations.

The URL Operating Phase experiments will address studies related to the emplacement and assessment of components of the disposal system (Simmons 1988).

No actual operating phase experiments have yet commenced but a trial exercise for an Operating Phase Excavation Response Experiment (ERE) has recently been conducted during the excavation of the 240 m level (Lang 1988). This 'small scale' excavation response "test" addressed excavation responses in terms of changes in the mechanical and hydrogeological conditions of the studied rock mass including a hydraulically conductive fracture, cf. Section 3.

This report addresses some issues raised with regard to observed discrepancies between the predicted and measured hydraulic responses in relation to this test. The present work constitutes the results of the work performed while the first author was an attached staff with the AECL/WNRE/URL as part of the joint AECL/SKB characterization program of the 240 m level at the URL.

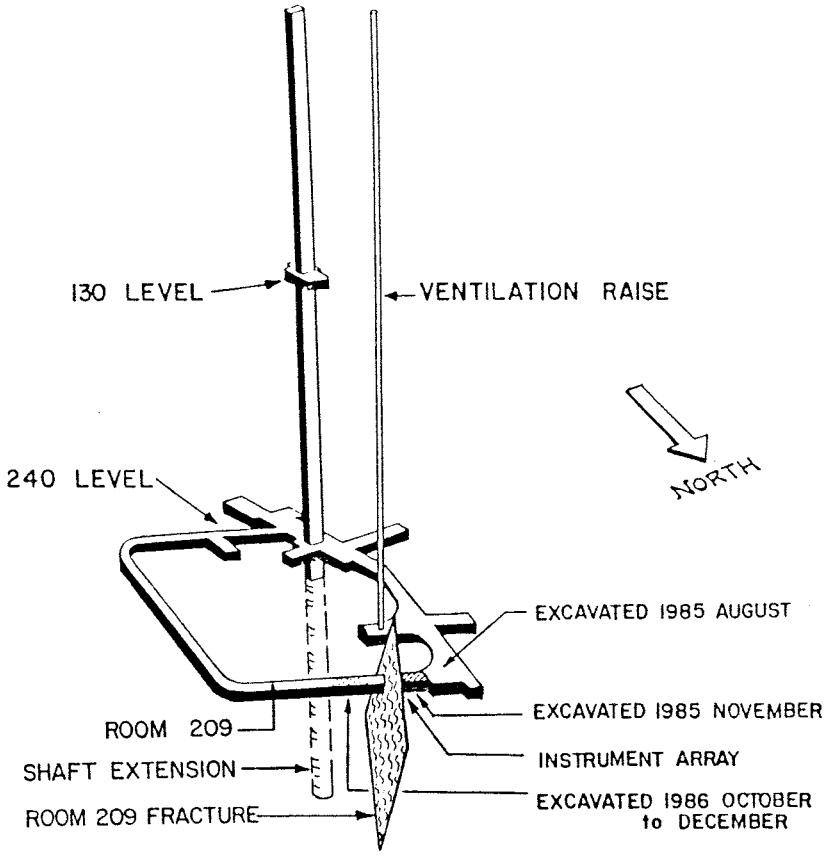

Figure 1.1 **Three-dimensional view of the URL showing the Room 209 extension and fracture.**

2. BACKGROUND

The Room 209 excavation response test at the 240 m level at the URL is set in an essentially unfractured part of the URL rock mass. The test was initially intended to constitute a purely mechanically oriented experiment. However, when the pilot hole of the planned extension of Room 209 intercepted a water bearing fracture (Lang et al 1988a) some 12 m ahead of the excavation face, the hydraulic aspects of excavation response in terms of the hydraulic response of the fracture was added. The experiment may be divided into five main phases:

I) Pre-characterization, including the installation of a instrumented array close to the noted fracture. Measurement of in-situ response during a short initial excavation section.

II) Pre-excavation model predictions of mechanical and hydraulic responses.

III) In-situ monitoring and collection of excavation response data when the tunnel was excavated through the instrumented fracture and rock mass.

IV) Post-excavation comparison and analysis of predicted and in-situ measured responses.

V) Post-excavation characterization and additional testing in the rock mass and fracture.

The Room 209 measurement array is presented in Figure 2.1. Notable is the fact that the array consists of two fans of boreholes. A radial fan (with respect to the tunnel axis) of 9 boreholes is positioned some four m before the tunnel intercept with the fracture. These boreholes are equipped with multi anchor extensometers. Subparallel to the tunnel axis 8 boreholes have been drilled, cf. Figure 2.2, hosting CSIRO triaxial strain cells at the very ends of the boreholes around 5 m ahead of the fracture. The borehole intercepts with the fracture are packed off with either AECL packer systems or Pac-ex instruments (Thompson et al 1988). These sections are all within 2 m of the final tunnel periphery. In addition a borehole was oriented to intercept the fracture some 13 m away from the tunnel towards the north.

The measured mechanical responses included monitoring of rock mass displacements, convergence and stress changes in the rock as the excavation successively proceeded. The measured hydraulic response in the fracture included monitoring of hydraulic pressure and measurements of groundwater inflow to the tunnel along the fracture trace, once penetrated, for each excavation stage (pilot and slash). In addition hydraulic single- or multi step drawdown tests were performed during the excavation process. The results of these tests were expressed in terms of changes in

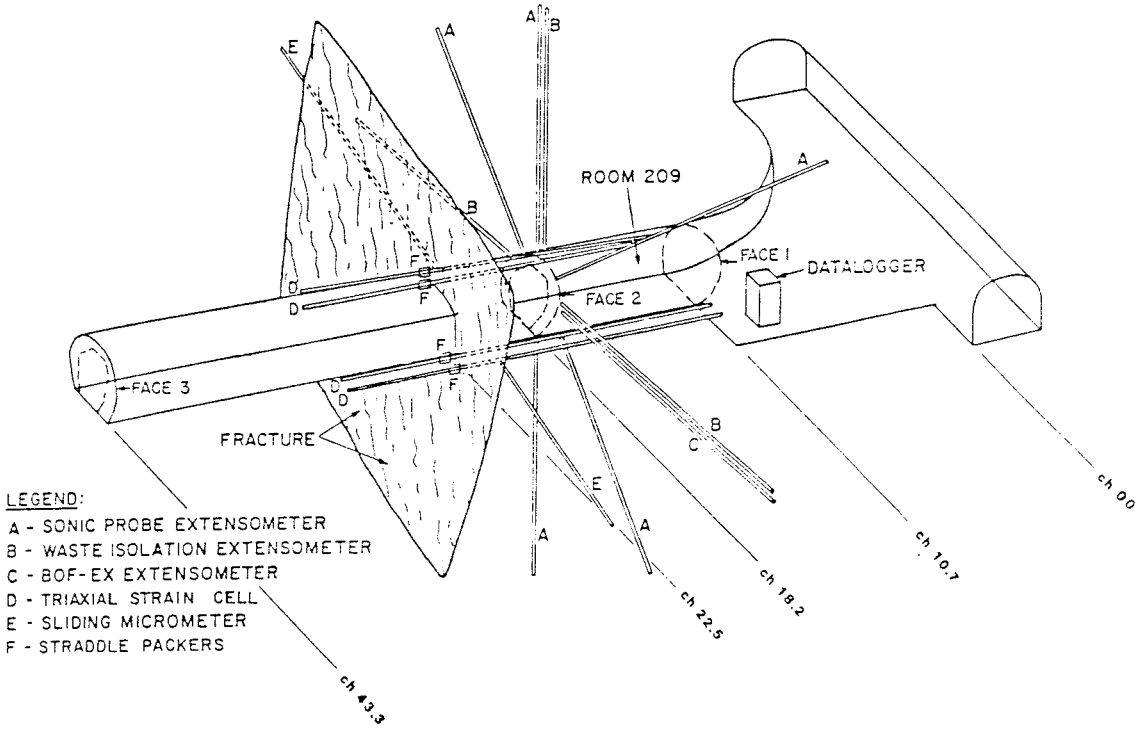

Figure 2.1 Perspective view of the Room 209 fracture and instrument array.

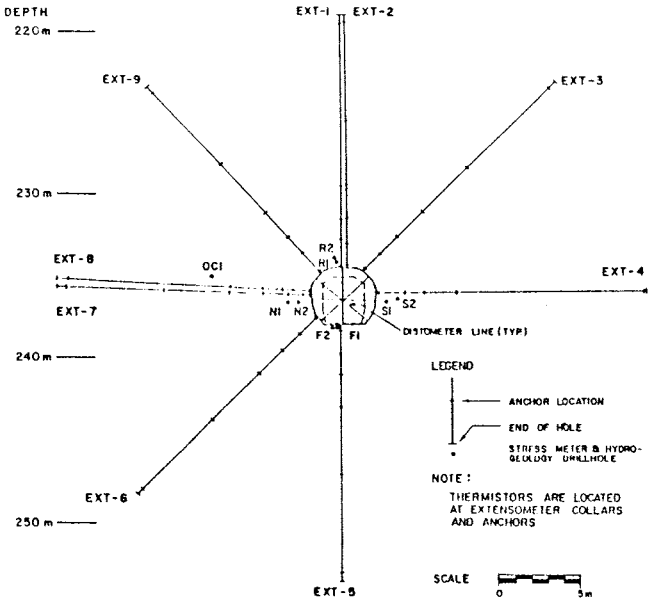

Figure 2.2 Vertical section through Room 209 showing the boreholes in the instrument ring.

normalized flow rate ($Q/\Delta H$) or as an equivalent single fracture aperture ($2b_{esf}$).

The data presented by Lang et al (1988a) constituted the only data supplied to the four modelling groups involved in the prediction modelling. The modelling predictions by AECL is presented by Chan et al in Lang (ed) (1988b). The AECL post-excavation comparison and back analysis is provided by Chan et al (1988).

The comparison and analysis is still underway. Draft reports presenting the results of the final phase indicate that the mechanical response at least trendwise has been accurately predicted (Chan et al 1988).

The hydraulic responses predicted include calculated head drop and inflow to the tunnel along the fracture trace for each excavation stage (pilot and slash). In addition an attempt was made with analytical techniques to predict the change in normalized flow rate resulting from changes in normal stress across the fracture (Chan in Lang et al 1988b).

A comparison between predicted and measured responses reveals that the calculated head drops are overpredicted by between one and two orders of magnitude and the inflow to the drift is over predicted by about one order of magnitude. The model calculations indicate a decrease in normalized flow rate in boreholes R1, F1

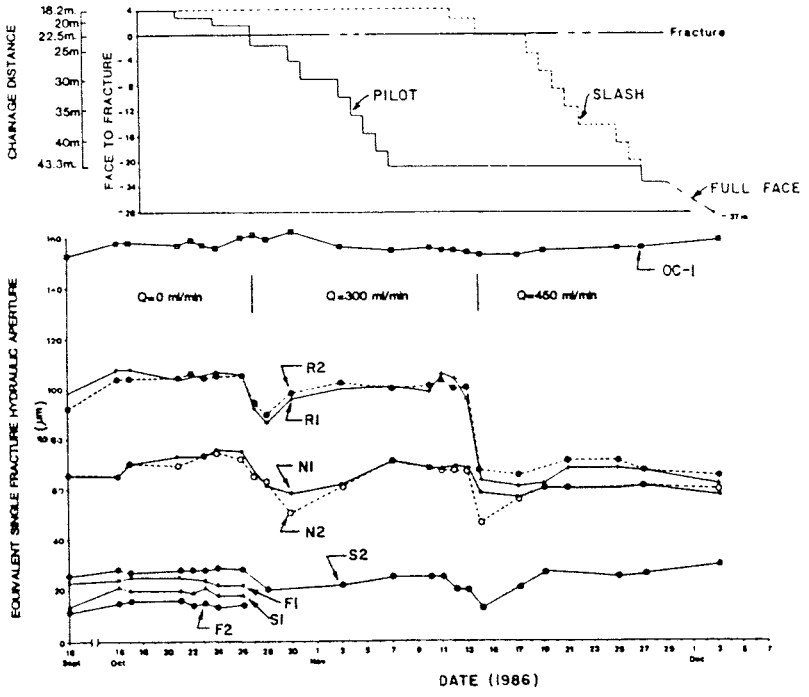

Figure 2.3 **Top: Advance of the pilot tunnel and slash vs. time, bottom: changes in equivalent single fracture aperture with time as inferred from drawdown test results (same time scale).**

and F2 by about 20% (pilot and slash response fairly equal) whereas the remaining boreholes close to the tunnel show increases by up to 40%. The noted changes (if due to changes in normal stress) are compatible with the noted changes in normal stress (< 2MPa) (Chan et al in Lang (ed) 1988b).

The in situ transmissivity measurements in trend indicate a decrease after the pilot followed by a recovery in the normalized flow rates almost to the initial values immediately before the slash intercept, cf. Figure 2.3. After the slash intercept a permanent decrease is noted (up to 80% in R1 and R2).

In Table 2.1 the results of the drawdown tests are presented as normalized flow rate for the different boreholes.

Table 2.1 Normalized flow rate $Q/\Delta H$ (m^2/s) as obtained from draw down tests in the Room 209 array. 1986 Sept 16 to 1986 Nov 27 data.

	BOREHOLE								
Date	N1 x10E-7	N2 x10E-7	OC1 x10E-6	R1 x10E-7	R2 x10E-7	F1 x10E-9	F2 x10E-9	S1 x10E-9	S2 x10E-8
16-Sep-86	1.71	1.71	2.19	5.93	4.74	7.58	1.04	1.61	1.11
16-Oct-86	1.68	1.68	2.40	7.60	6.75	8.70	2.20	5.10	1.30
17-Oct-86	2.04	2.04	2.40	7.58	6.87	9.10	2.40	4.97	1.18
21-Oct-86	2.37	1.99	2.35	6.83	6.83	9.87	2.53	4.85	1.23
22-Oct-86	2.37	2.21	2.45	6.94	7.18	*	1.59	4.19	1.26
23-Oct-86	2.37	2.37	2.36	5.59	6.90	8.70	2.17	5.07	1.31
24-Oct-86	2.70	2.42	2.28	7.35	6.94	6.64	1.35	3.79	1.42
26-Oct-86	2.51	2.25	2.46	7.23	6.99	6.40	1.52	3.79	1.28
27-Oct-86	1.84	1.69	2.51	4.74	5.02	-	-	-	-
28-Oct-86	1.34	1.50	2.44	3.84	4.24	-	-	-	0.48
30-Oct-86	1.20	2.66	2.60	5.29	5.69	-	-	-	-
03-Nov-86	1.42	1.33	2.29	6.06	6.42	-	-	-	0.64
07-Nov-86	2.14	2.14	2.25	6.26	6.26	-	-	-	0.92
10-Nov-86	1.89	1.89	2.28	5.85	6.30	-	-	-	0.94
11-Nov-86	1.87	1.82	2.24	7.11	6.56	-	-	-	0.92
12-Nov-86	2.02	1.80	2.26	6.80	6.04	-	-	-	0.45
13-Nov-86	1.87	1.80	2.22	5.17	5.97	-	-	-	0.46
14-Nov-86	1.19	0.60	2.18	1.51	1.80	-	-	-	0.15
17-Nov-86	1.11	1.07	2.16	1.39	1.67	-	-	-	0.52
19-Nov-86	1.28	1.28	2.24	1.42	1.42	-	-	-	1.19
21-Nov-86	1.29	1.29	*	1.92	2.14	-	-	-	*
25-Nov-86	1.30	1.30	2.28	1.89	2.16	-	-	-	0.92
27-Nov-86	1.38	1.38	2.32	1.78	1.78	-	-	-	1.02
Zone Length m	0.69	0.69	1.00	1.00	1.00	2.50	2.50	1.50	1.50

- no flow
* poor test

In the post-excavation analysis performed by Chan et al (1988) the effects caused by the internal atmospheric boundary along the excavation periphery on the results of the simulated single-hole drawdown tests were studied. In the process the hydraulic model was made more refined and all boreholes apart from boreholes OC1, F1 and F2 were explicitly represented. No changes of the model geometry or external boundary conditions were undertaken. **It was found that the internal boundary effect, possible effects of changes in normal stress and other possible changes in material properties excluded, could not explain the noted permanent decrease in in-situ measured normalized flowrate.**

The current study which is part of the post-excavation comparison and analysis process is addressing the following issues:

* Revision of the model geometry using all data available at 1988 March.

* Revision of the external boundary conditions of the model making use of all data available at March 1988.

* Calibration of pre-excavation model performance against in-situ data.

* Analysis of post-excavation (pilot included) model behaviour when appropriate boundary conditions are applied to the calibrated pre-excavation model.

* Seek possible explanations to observed discrepancies between in-situ and modelled response.

3. CONCEPTUAL MODEL

3.1 Basic assumptions

The results of the pre-excavation characterization undertaken to provide the different modelling teams with basic information showed that the Room 209 fracture, rather than being a discrete fracture, in fact is a zone containing 1 to 6 fractures, (Everitt in Lang et al 1988a). In addition the width of the Room 209 fracture is widening according to Everitt (pers. comm.) from a few decimeters close to Room 209 to about 0.9 metres where 209-010-OC1 intersects the fracture. According to preliminary interpretations of data from a new probe hole (209-059-PH3) extending north from the end of the Room 209 extension, cf. Figure 3.1, the width of the zone at an approximate distance of 100 m is on the order of 5 metres (Everitt, pers. comm.). Everitt further schematically outlines a wedge or "semi-canoe" fracture zone shape. The intercept of the fracture with the room extension is at the extreme south edge of the feature, cf. Figure 3.2.

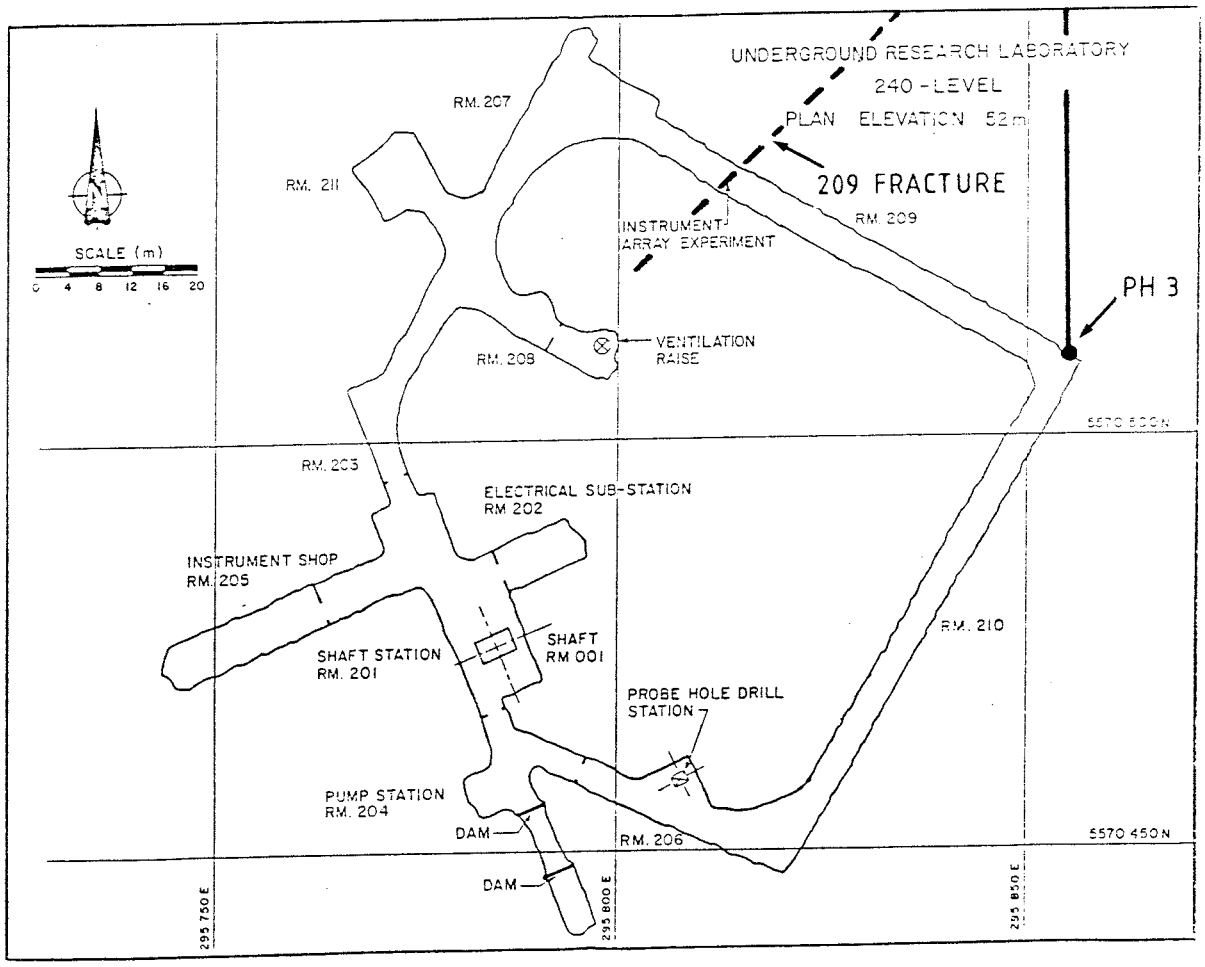

Figure 3.1 Plan view of the 240 m level.

However, despite the fact that a number of arguments contradicts the adaption of a single parallel plate fracture, the parallel plate approach has been taken. This mainly because of the lack of a more detailed geometrical and hydraulic description in the fracture to the north. In addition no hydraulic communication between the fracture and the surrounding rock is assumed.

In the present modelling work, only steady state fluid flow calculations have been performed. Transient calculations have not been performed since previous analysis by Chan et al (in Lang et al 1988a) showed that steady state conditions were obtained within a short time.

3.2 Geometry of the fracture

In the previous modelling of the fracture hydrology performed by Chan et al (in Lang et al 1988b) and Chan et al (1988) a fixed model geometry has been used based on the information that was provided to the modelling teams prior to start of excavation.

In the current modelling exercise (being part of the post excavation analysis) an attempt has been made to make use of any new information collected during the excavation process and later stages that can add to the geometrical and hydrogeological conceptualization of the fracture.

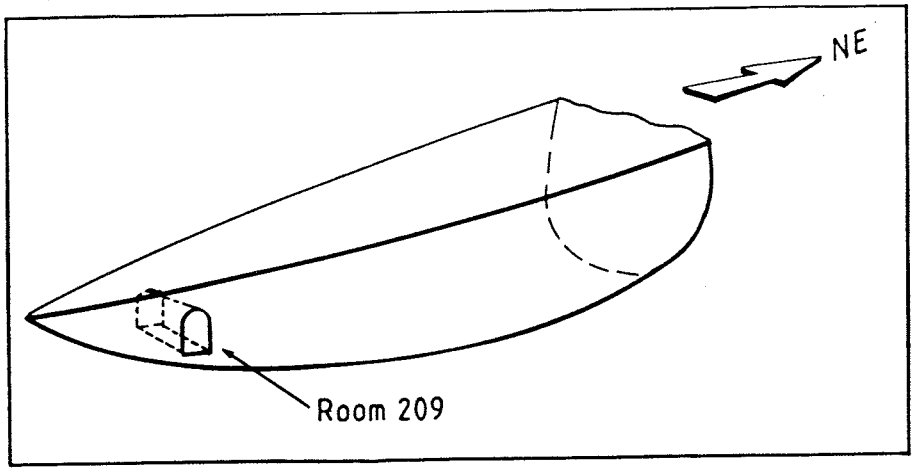

Figure 3.2 **Schematic conceptual model of the shape of the Room 209 fracture (Everitt, pers. comm. 1988).**

In this respect the new borehole 209-059-PH3 has added a new understanding of the extent of the fracture to the north, i.e. the fracture extends at least to the point of intercept with borehole 209-059-PH3. This fact is also substantiated by hydraulic observations in the Room 209 array during drilling of this borehole, (Kozak, pers. comm.).

The extent towards the south has been a topic of debate with regard to boundary conditions. This analysis presented in Section 3.4 substantiated the extent assumed by Chan et al (in Lang et al 1988b and 1988) which is some 15 metres south of the tunnel periphery.

The vertical extent has been kept unaltered with respect to the assumptions made by Chan et al (in Lang et al 1988b) and Chan et al (1988), i.e. the fracture is assumed to extend to the lower horizontal boundary of Fracture zone 2.5, cf. Figure 3.3.

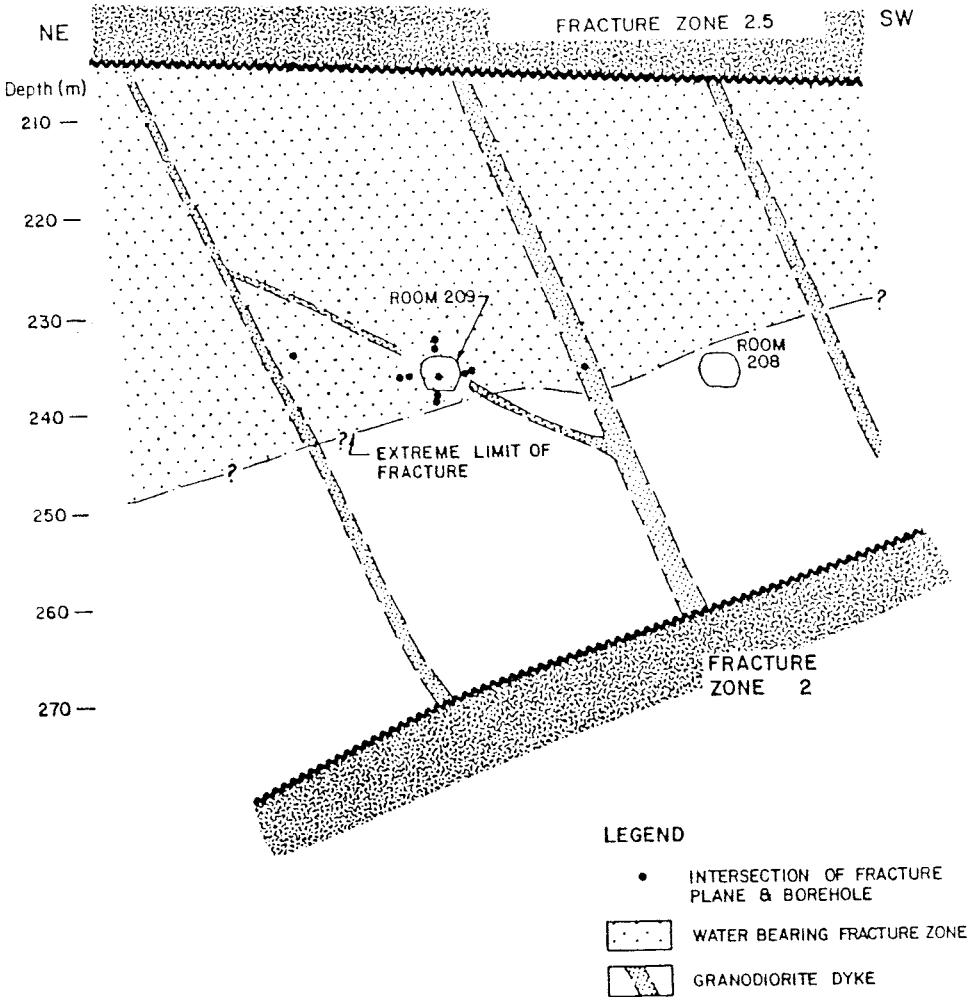

Figure 3.3 **Conceptual model of the geology of the Room 209 fracture and its environment. View in the fracture plane (Everitt in Lang et al 1988c).**

The lower bound of the fracture was assumed by Chan et al (in Lang et al 1988b) and Chan et al (1988) to be horizontally positioned some 8 m below the floor of the drift along the fracture plane. In the new geometrical description the updated geometry provided by Everitt (in Lang et al 1988c) has been used, cf. Figure 3.3. The lower hydraulic bound is here interpreted as the upper bound of the noted alteration halo which is associated with a lowered permeability at the assumed physical lower bound of the fracture. The lower bound of the fracture has consequently been described as a gently inclined linear feature over the lateral extension of the fracture.

A granodiorite dike crosses the tunnel cross section as shown in Figure 3.3. This feature is also interpreted as a low permeability portion of the model, cf. Section 3.3.

3.3 Material property distribution

The material property distribution can roughly be divided into three major subparts, cf. Figure 3.4:

1) Tunnel area which covers the area subject to detailed testing close to the periphery of the 209 extension.

2) Near field which covers the remaining parts of the old fracture model (Chan et al (in Lang et al 1988b) and Chan et al 1988) including the influence area of testing in 209-010-0C1.

3) Far field which makes up the extended part of the model to the north, beyond the old northern vertical bound.

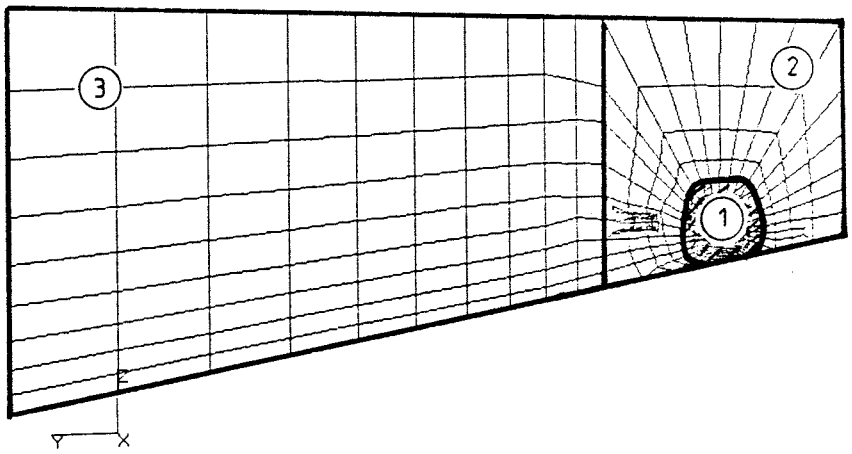

Figure 3.4 **Large scale regions in terms of material properties in the revised Room 209 fracture hydraulic model. 1=tunnel area, 2=near field, 3=far field.**

For the initial material property distribution in the tunnel area, use has been made of data on the distribution of equivalent single fracture aperture ($2b_{esf}$) provided by Kozak in Lang et al (1988a), cf. Table 3.1. In this context the Oct 16 data of 1986 was considered representative of the pre-excavation conditions. The aperture was recalculated to a fracture permeability (K_{fr}) for each borehole location. The assumed influence radius/area of the testing performed in each borehole, thus representing the values obtained, are presented in Figure 3.5. There are no direct quantitative data on the permeability of the granodiorite dike. However, qualitative information from the interference tests performed within the borehole array has provided information on its permeability relative to the neighboring constituents.

Apart from the test results for borehole 209-010-OC1, cf. Figure 2.2, no additional hydraulic data are available for the near field. Consequently the whole near field region has been assigned the properties obtained from testing of 209-010-OC1. No testing whatsoever has been conducted in the far field region thus far. However, the inflow and pressure readings recorded during the packer installations in 209-059-PH3 (Kozak, pers. comm.) have been used to infer a tentative equivalent single fracture permeability for this region.

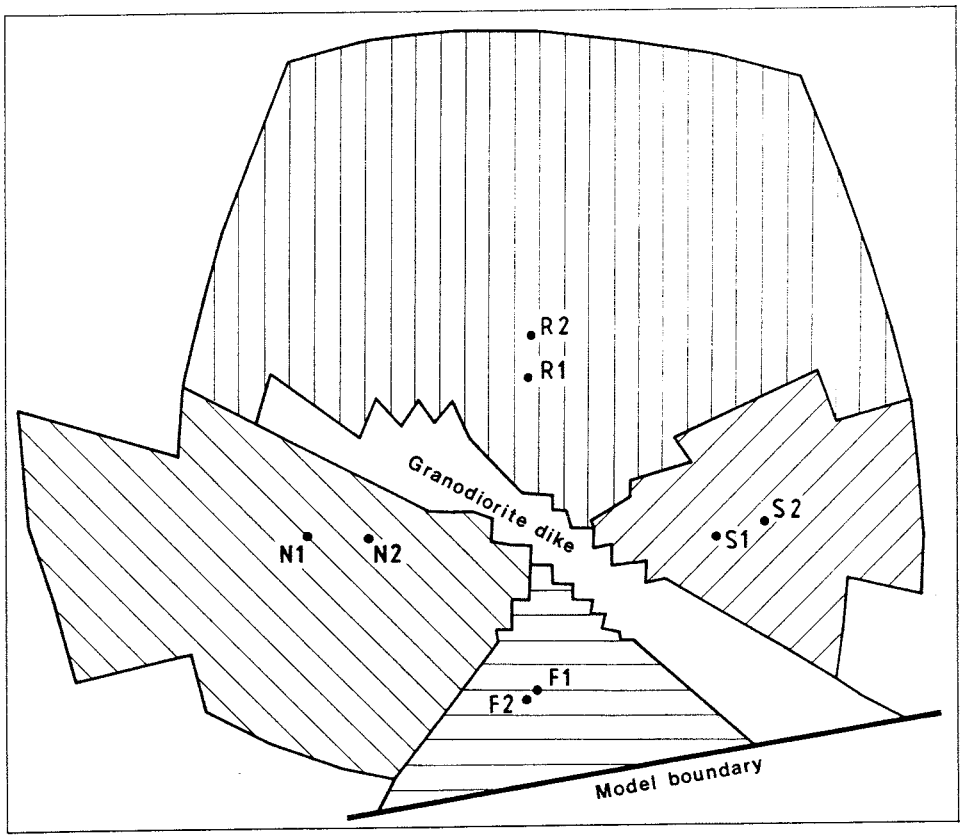

Figure 3.5 **Close-up of tunnel area (1) indicating the influence areas of the four pairs of boreholes close to the periphery of the pilot drift.**

3.4 Boundary conditions

In previous modelling exercises that focused on the Room 209 fracture (Chan et al in Lang et al 1988b and Chan et al 1988) no flow boundaries were assumed along the vertical faces of the model and also along the lower horizontal boundary. The upper horizontal boundary along the lower bound of Fracture zone 2.5 was assumed to be a constant head boundary defined by the recorded pressures in the boreholes around the tunnel.

Within the scope of the post excavation analysis the present modelling includes a review of the boundary conditions applied. Some questions have been raised with respect to the validity of an assumed vertical no flow boundary in the south as far off as 15 metres from the drift periphery. Discussion and analysis of material provided by Ed Kozak (pers. comm.) regarding observed waterbearing features in extensometer boreholes drilled to the south sustained the positioning of the south boundary. The lower boundary is still considered as a no flow boundary but with the geometry outlined in the previous section.

The addition of pressure readings in the newly instrumented borehole 209-059-PH3 casts new light on the boundary conditions along the upper horizontal bound. Pressure readings in this borehole from late 1987 to April 1988 is presented in Figure 3.6. In late March the pressure in the sectioned off zone encompassing the Room 209 fracture show a pressure of approximately 1475 kPa (Head H=204 m a s l, corrected for atmospheric). At the time when pre-excavation conditions prevailed, late fall 1986,

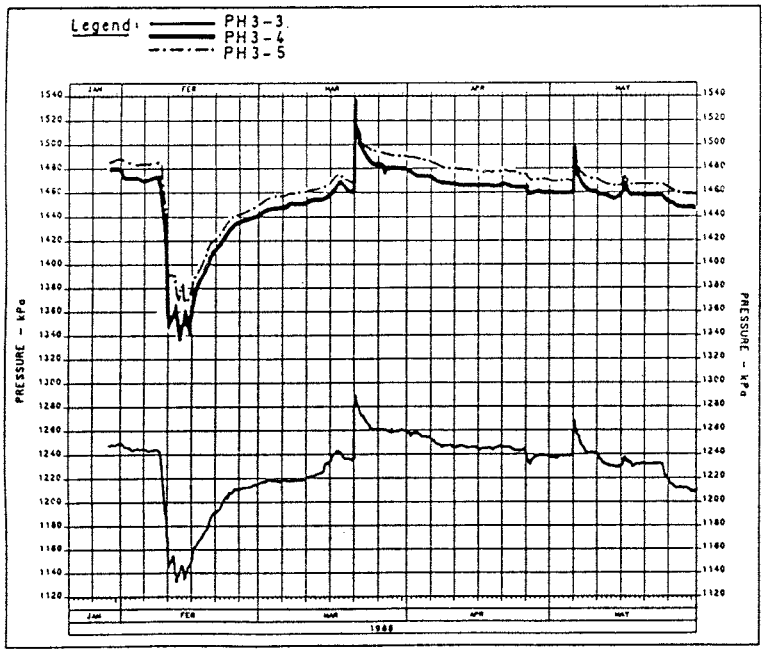

Figure 3.6 **Pressure recorded in borehole 209-059-PH3. Zone 4 corresponds to the interpreted occurrence of the Room 209 fracture in this borehole at borehole length L=95 m.**

borehole 209-010-OC1, cf. Figure 2.2, show a pressure of approximately 1090 kPa (Head H=157 m a s l). The major drawdown event acting on the fracture in this region at the time was the newly developed vent raise positioned some 25 m south of the tunnel. The fact that OC1 showed a minor response to the excavation process and the fact that a point corresponding to the PH3 intercept must have had a pressure at least in excess of the March 1988 reading suggests that an inherent hydraulic driving force acted in the fracture prior to start of the excavation. This gradient corresponding to a head drop of 47 metres over a horizontal distance of 80 m has been incorporated into the model in the far field, cf. Figure 3.7. For the near field a constant head H=152 m a s l has been assumed along the upper horizontal face.

The vertical face in the north has been assigned a constant head boundary condition of H=204 m a s l because the extent of the fracture beyond this point is not clearly established.

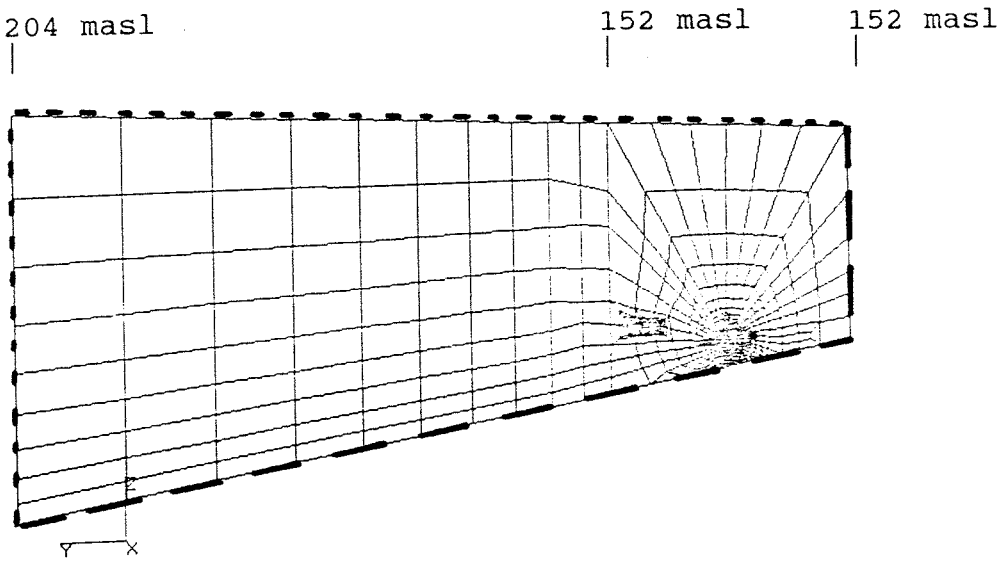

Figure 3.7 Boundary conditions applied to the revised Room 209 fracture hydraulic model.
--- Q=0, ... Φ=const.

4. MODELLING SPECIFICS

4.1 Pre-processing and topology

The Finite Element mesh constructed by Chan et al (1988) was the base which was altered according to the changes described in Section 3.2. The original mesh contains the two-dimensional fracture suspended with its interpreted geometry in the three-dimensional space.

Apart from the purely geometrical changes carried out, a more refined discretization was performed around the locations of the F-family of boreholes, cf. Figure 4.1, boreholes 209-010-OC1 and 209-036-OC1. The latter borehole was drilled and instrumented after the tunnel and slash were excavated. By using the pre-processing capabilities of PATRAN (PDA Engineering 1985) the nominal diameter of the boreholes was described explicitly (ϕ=0.096m).

The resulting Finite Element mesh contains 1438 2D quadrilateral elements and a total of 1502 nodes, cf. Figure 3.7.

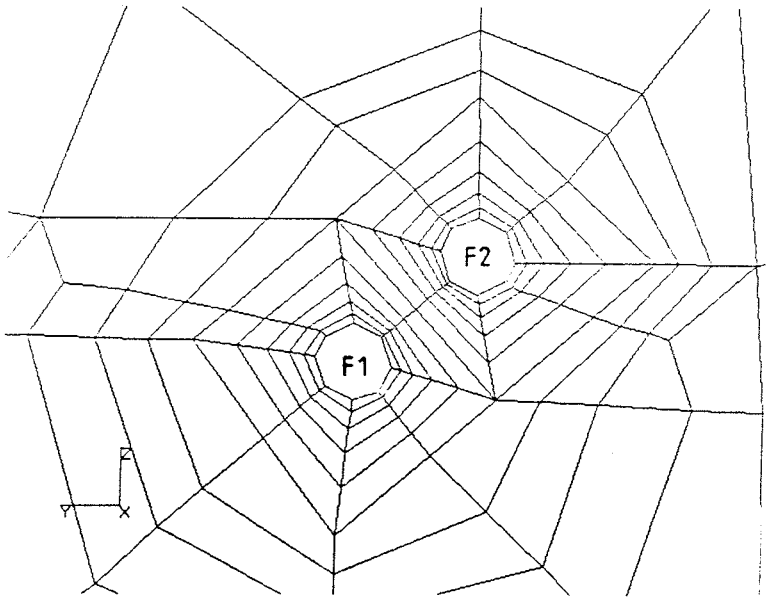

Figure 4.1 **Close-up on the discretization of boreholes F1 and F2. The nominal diameter of the boreholes is 0.096 m.**

4.2 Code used

The computer code MOTIF developed by AECL (Guvanasen 1984) has been used to simulate the groundwater flow conditions in the fracture. MOTIF is a three-dimensional finite element computer code that solves the steady and transient state equations of groundwater flow, heat transfer and radionuclide transport for a continuous porous medium.

As already pointed out, the present modelling work only constitute steady state fluid flow calculations since previous results (Chan et al in Lang et al 1988b) showed that steady state was obtained within a very short time.

4.3 Post-processing

In order to facilitate calculation of reactive recharge to a set boundary condition, on a borehole surface or the surface of an underground opening, use has been made of a routine that calculates the flux over a specified element surface. The flux is obtained by integrating the normal component of the velocity vector over the relevant element boundaries.

The presented calculated head values at borehole intercepts with the Room 209 fracture are the mean values of the 8 to 10 nodal points corresponding to the element faces delineating the crossection of each borehole, cf. Figure 4.1.

4.4 Organisation of presentation of model results

The pre-excavation model is calibrated in three steps representing three model generations I-III. The post-excavation conditions is analysed in one model generation (IV) which does not take skin effects into account and a second generation (V) which take into account different scenarios of skin around the tunnel opening. The different model generations and the models run are presented in Table 4.1 together with references to the relevant sections of the report.

Table 4.1 Organization of presentation of model results

Model	Generation	Excavation state	Report section	Comments
FRACT8A	I	pre-	5.2	
FRACT8B	II	pre-	5.3	
FRACT8C	III	pre-	5.4	final
FRACT8E	IV	post-	6.2	no skin
FRACT8F	V	post-	6.3	with skin

5. SIMULATION OF PRE-EXCAVATION CONDITIONS

5.1 General

This section describes the computer runs performed to simulate the conditions prevailing in the fracture prior to start of the extension of Room 209. For the 3 model generations studied (I, II and III) the undisturbed steady state head distribution (corresponding to no testing being performed) has been calculated. In addition the simulation of multi-step drawdown tests have been performed for each borehole.

The geometry and boundary conditions of the models A-C are all the same. The only free parameter is the fracture permeability (or, equivalently, the aperture of the fracture).

5.2 Model generation I (FRACT8A)

5.2.1 Steady state head distribution

This model corresponds to the 1986 Oct 16 data with regard to material properties, cf. Figure 5.1 and Appendix 1. The calculated steady state head distribution in the simulated boreholes is presented in Table 5.1 together with the in-situ measured head prior to excavation. The calculated head values for the FRACT8A model are within 7% of the in-situ measured ones.

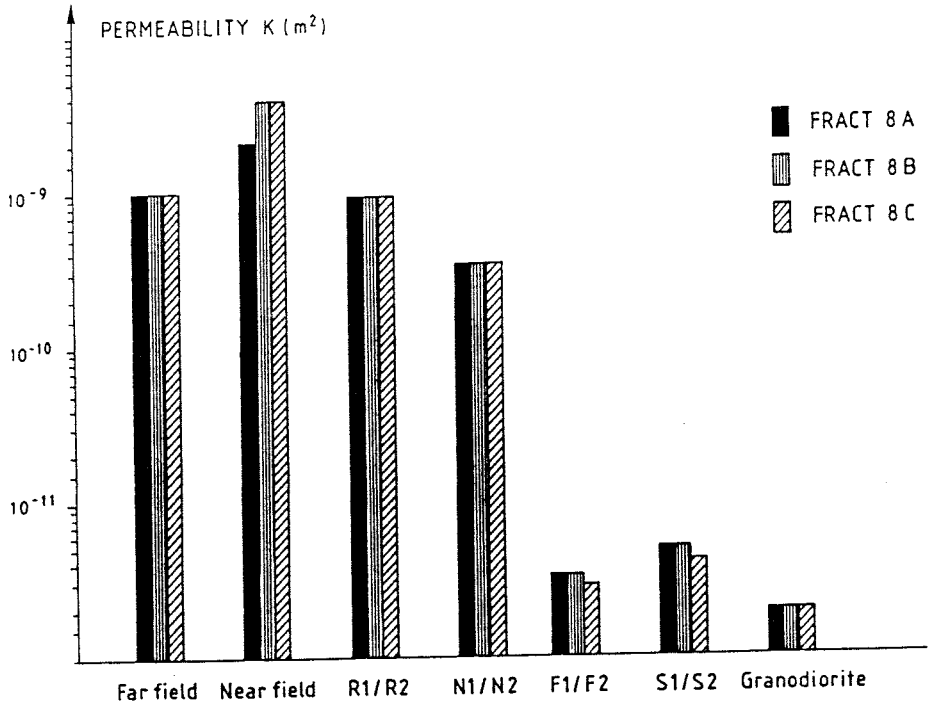

Figure 5.1 **Input material properties to models used to simulate the pre-excavation hydraulic conditions in the Room 209 fracture, cf. Figures 3.4 and 3.5.**

Table 5.1 **Calculated steady state head at each borehole location in the Room 209 array for model generation I-III and the corresponding in-situ measured hydraulic head.**

Borehole	Hydraulic head (masl)*)			
	In-situ measured	Calculated FRACT8A	Calculated FRACT8B	Calculated FRACT8C
OC1	156.2	157.9	155.1	155.1
N1	150.5	157.2	154.8	154.8
N2	153.0	157.2	154.8	154.8
F1	147.1	156.9	154.6	154.6
F2	152.1	157.0	154.6	154.6
R1	155.1	155.0	153.5	153.5
R2	153.7	155.0	153.5	153.5
S1	152.7	154.5	153.2	153.2
S2	149.3	154.3	153.1	153.1

*) corrected to zero pressure at the land surface.

5.2.2 Simulation of single hole drawdown tests

This part of the calculation process involved the simulation of the drawdown tests that were performed prior to excavation. Though some field tests were multi-step and some single step, all tests in model generation I have been simulated using three different head drops (ΔH=2, 5 and 10 metres). The results of the simulation, presented in terms of normalized flow rate ($Q/\Delta H$), are given in Figure 5.2 and Appendix 2.

The results of the simulated testing showed that a linearity in $Q/\Delta H$ prevailed in all boreholes for the drawdown interval chosen. This fact is only natural since the system of differential equations is linear. In addition the calculated normalized flow rates were within 75% of the measured ones for all boreholes but OC1 which was off by a factor of 2.6. Most discrepancies represent underestimations including the results of the simulation of the OC1 tests.

5.2.3 Conclusions

With:

a) the assumed geometry of the model
b) the assumed influence areas of the borehole tests
c) the assumed boundary conditions, and
d) the assumed 1986 Oct 16 input permeabilities

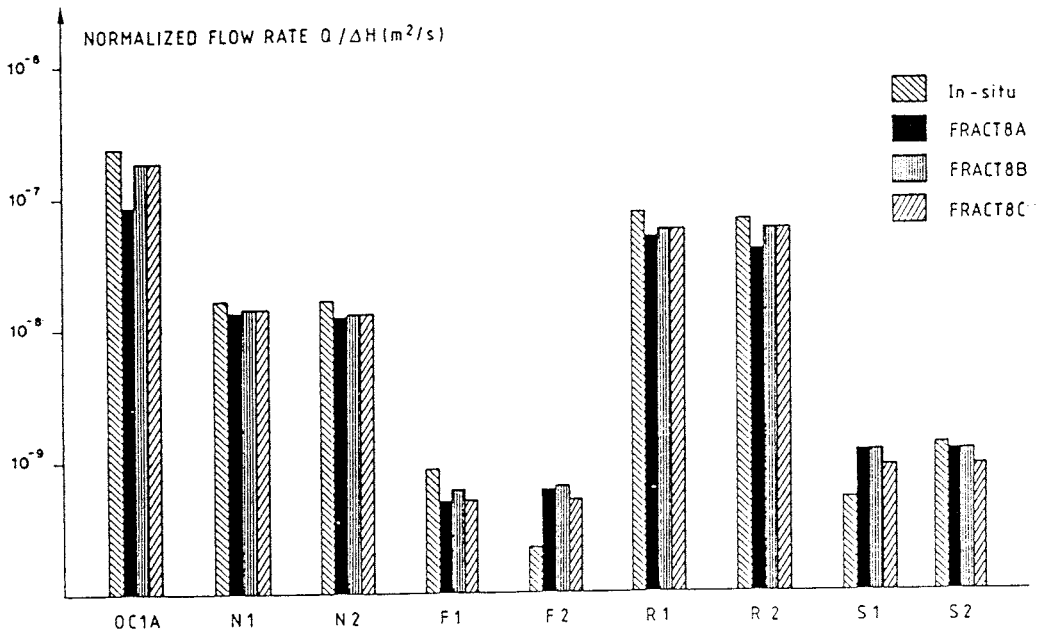

Figure 5.2 **Results from in-situ and simulated drawdown tests in boreholes in the Room 209 instrument array during pre-excavation conditions.**

the model suffices to reproduce the measured normalized drawdowns within 75% in all boreholes but one (OC1) which is off by a factor 2.6. In addition the steady state head at the borehole intercepts are overestimated within 7%. That means that the model is a reasonable realization of the in-situ conditions for the loads applied and conditions assumed.

5.3 Model generation II (FRACT8B)

5.3.1 Simulation of steady state head distribution

This model denoted FRACT8B is identical to FRACT8A apart from the fact that the permeability in the near field region has been increased by a factor 1.8 to $3.8 \cdot 10^{-9}$ m^2, cf. Figure 5.1 and Appendix 1. This is to allow a higher yield of water into the area influenced by the boreholes and at the same time supply a relief in calculated head in the area close to the tunnel.

The calculated steady state head at the borehole intercepts for this model range from 153.1 (S2) to 155.1 m a s l (OC1), cf. Table 5.1. The values are all within 5% of the in-situ measured head. This is a slight improvement when compared with model generation I.

5.3.2 Simulation of single hole drawdown tests

Since linearity in Q vs. ΔH has been established for model generation I and only minor changes with regard to material properties had been undertaken, only a drawdown of ΔH=5 m was used in the simulations based on the FRACT8B model.

The results indicate, cf. Figure 5.2 and Appendix 2, that the model produces a higher normalized flow rate than model generation I, e.g. OC1 is underestimated within 30% compared to an underestimation with a factor 2.6 in FRACT8A.

5.3.3 Conclusions

The model reproduces the tests with an acceptable correspondence given the assumptions made. At this point it did not seem relevant to pursue the fitting of parameters to the measured results further. This argument is based on:

a) the inherent ambiguity in solution of the inverse problem.

b) the adaption of parallel plate approach although the fracture is undoubtedly made up of more than one fracture.

However, one final set of runs was decided upon to obtain a better distribution in the discrepancy in the match between calculated and measured $Q/\Delta H$ for the F and S pair of boreholes.

5.4 Model generation III (FRACT8C)

5.4.1 Simulation of the steady state head distribution

This model, denoted FRACT8C, is identical to FRACT8B apart from the fact that the permeability in the F1/F2 and S1/S2 influence areas have been decreased by a factor 0.84 and 0.83, respectively, cf. Figure 5.1 and Appendix 1.

The results of the calculation, cf. Table 5.2, indicate that the steady state head calculated are unchanged when compared to the calculations based on FRACT8B, i.e. the head are within 5% of the measured ones.

5.4.2 Simulation of single hole drawdown tests

The results of this model based on head drops ΔH of 5 m are comparable to the results based on FRACT8B apart from some minor differences for the F and S pair of boreholes, cf. Figure 5.2 and Appendix 2. As a result all boreholes show results within 75% of the in-situ measured normalized flowrates.

Table 5.2 **Simulated crosshole hydraulic interference tests in the Room 209 instrument array. The ratio $\Delta H_i/\Delta H_o$ is presented for the calculated data and for field data (second line for each test) where available. ΔH_o and ΔH_i refers to the head drop in the active and observation well, respectively.**

Obs. well	Active well in fracture								
	OC1	N1	N2	F1	F2	R1	R2	S1	S2
OC1		0.04	0.04	0.01	0.01	0.06	0.08	0.01	0.01
		0.05	0.05	0.01	-	0.10	0.08	-	-
N1	0.60		0.44	0.02	0.02	0.10	0.10	0.01	0.01
	0.88		0.93	0.03	-	0.14	0.12	-	-
N2	0.60	0.52		0.02	0.02	0.10	0.10	0.01	0.01
	0.88	0.92		0.03	-	0.14	0.10	-	-
F1	0.56	0.28	0.34		0.64	0.14	0.14	0.04	0.04
	0.76	0.68	0.69		-	0.20	0.18	-	-
F2	0.56	0.26	0.32	0.62		0.12	0.12	0.04	0.02
	0.75	0.66	0.60	0.92		0.19	0.17	-	-
R1	0.30	0.02	0.02	0.01	0.01		0.64	0.01	0.01
	0.70	0.05	0.05	0.01	-		0.52	-	-
R2	0.30	0.02	0.02	0.01	0.01	0.60		0.01	0.01
	0.70	0.05	0.06	0.02	-	0.60		-	-
S1	0.24	0.02	0.04	0.02	0.01	0.30	0.28		0.32
	0.32	0.01	0.00	0.00	-	0.41	0.36		-
S2	0.22	0.02	0.02	0.01	0.01	0.24	0.24	0.30	
	0.68	0.01	0.05	0.00	-	0.54	0.48	-	

5.4.3 Simulation of multiple hole interference tests

The collected data from the FRACT8C runs may be used to infer also the crosshole responses due to an applied pressure drop in a single borehole. The ratio $\Delta H_i/\Delta H_o$ for the calculated data can in this context be compared with the in-situ measured quantity supplied by Kozak in Lang et al (1988a). ΔH_i refers to the observed head drop in an observation well whereas ΔH_o is the head drop in the active well. The results, compiled in Table 5.2 and graphically presented in Figure 5.3, indicate that the observed responses, where comparison with field data is possible, though not accurate in absolute magnitude, describe the relative magnitude reasonably well. Most values are within a factor 2.5 of the observed ratio. However, the R family of boreholes show a very good agreement with field data.

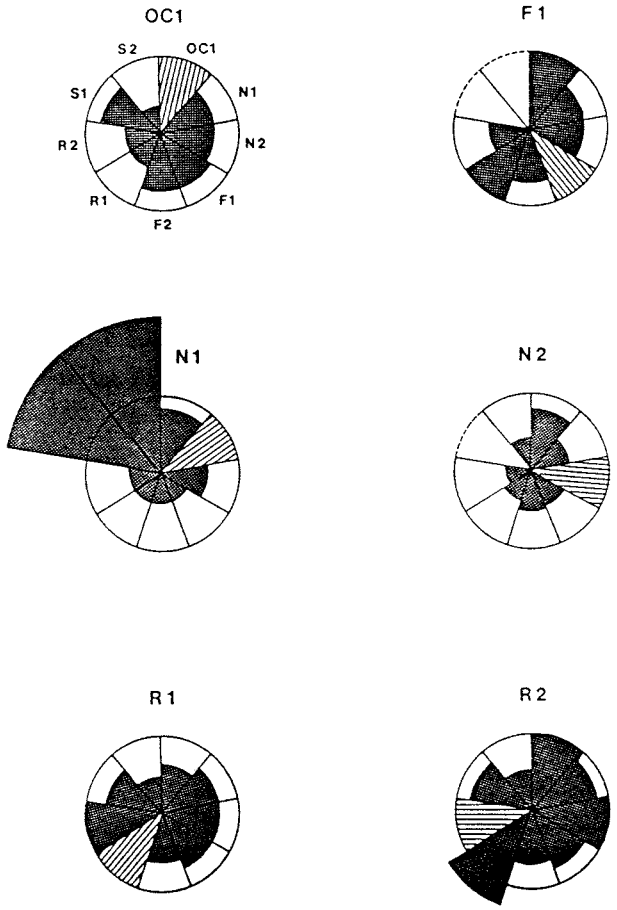

Figure 5.3 Simulation of hydraulic interference tests in the Room 209 instrument array. $\Delta H_i/\Delta H_o$ for the different simulated tests normalized to (i.e. divided by) the corresponding quotient based on the field results. Boreholes F2, S1 and S2 are lacking due to absence of field results, cf. Table 5.2. Circle = unit circle = exact agreement.

6. SIMULATION OF POST-EXCAVATION CONDITIONS

6.1 General

This section describes the simulation of the hydraulic conditions after the excavation of the pilot tunnel through the fracture. The effects are accounted for in terms of changes in steady state head in the boreholes in the array, inflow along the fracture trace into the tunnel, and finally changes in calculated normalized flowrate when the drawdown tests are repeated in the boreholes.

Four cases are considered, FRACT8E (IV), which describes the response to the pilot with unaltered material properties (identical to pre-excavation conditions, FRACT8C) and a generation of models which address possible skin around the pilot excavation, FRACT8F (V) (3 cases).

The calculation process is identical to the one used to describe the pre-excavation conditions.

6.2 Model generation IV (FRACT8E)

6.2.1 Simulation of head drop and inflow due to pilot

This model, denoted FRACT8E, is identical to FRACT8C apart from the fact that the pilot crossection, cf. Figure 6.1 and Table 6.1, has been assigned a permeability k=1 and that atmospheric pressure boundary conditions have been prescribed to the surfaces of the pilot.

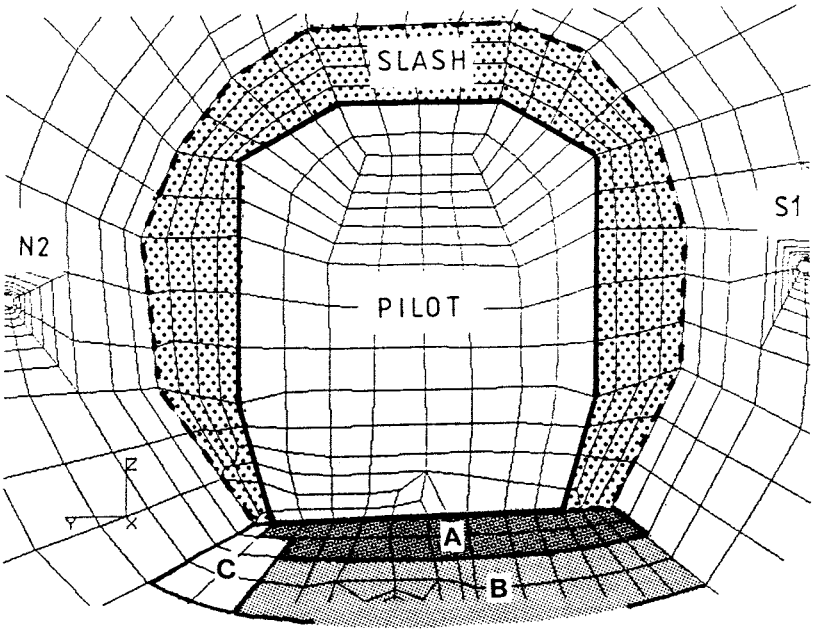

Figure 6.1 Close-up of the drift area indicating the subareas where changes in permeability have been applied.

The calculated head in the boreholes varied from 68.2 (F1) to 145.4 m a s l (OC1). The head drops ΔH in relation to the FRACT8C results varies between 9.7 (OC1) to 86.4 m in F1, cf. Table 6.2 and Figure 6.2. In comparison to the in-situ measured results the calculated drawdowns are overestimated up to 30 times. A notable exception is the F family of boreholes where the head drop is underestimated by 20%.

The calculated inflow to the tunnel along the fracture trace amounts to 4.53 l/min. Of this inflow, 82% emanates from the roof whereas 15% enters along the north wall. Only 2% enters through the floor, c.f Table 6.3.

6.2.2 Simulation of single hole drawdown tests

In the simulation process, head drops ΔH of 5 m have been used. The calculated normalized flowrates are presented in Table 6.4 and Figure 6.3. A direct effect of the incorporation of the pilot in this case is that up to 50% of the model element surfaces delineating each individual borehole show fluxes out of the borehole into the adjacent rock. The element surfaces in question are facing the tunnel and indicate the superimposed effect that the excavation has on the simulated test. Between 1.5 and 14% of the absolute values of the net flow is out of the borehole during a simulated drawdown test.

The FRACT8E model underpredicts the normalized flow rate in OC1 by 20% compared to the measured value, cf. Table 6.4. The remaining boreholes, apart from the F family, show an overprediction by up to 40%. This result despite the fact that fluxes out of the borehole occur. This finding is consistent with the results regarding the internal boundary effect presented by Chan et al (1988).

A comparison between the pre- and post-excavation modelling results yields that the FRACT8E model predicts an increase in normalized flow rate of 0-37% as a result of the pilot tunnel intercept, cf. Table 6.5.

6.2.3 Conclusions

The drawdown in FRACT8E at the borehole intercepts with the fracture, apart from F1 and F2, has been overestimated by one to two orders of magnitude. A coupled effect is that the inflow to the drift has been overestimated by more than one order of magnitude. The relative distribution of the inflow also indicates that the roof contributes 82% of the inflow.

Present understanding of the changes in stress over the Room 209 fracture and the normal stiffness of the fracture suggest that stress induced permeability changes play a subordinate role in explaining differences between in-situ measured and calculated responses (head drops, inflow to tunnel and hydraulic test

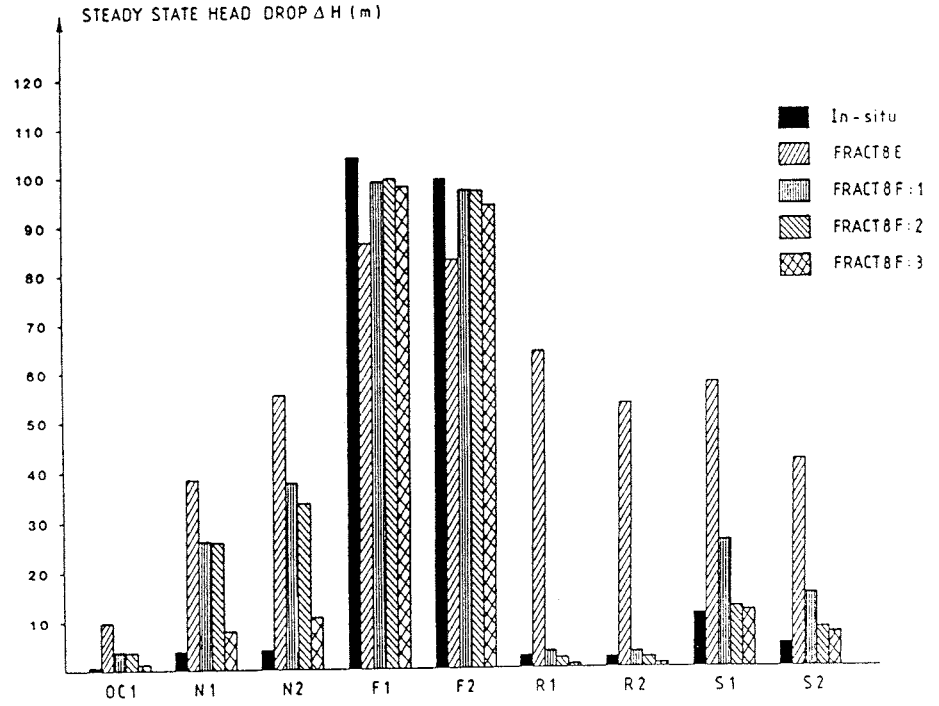

Figure 6.2 Graphical representation of calculated and measured head drop in the boreholes following the intercept of the pilot tunnel with the fracture.

results) due to the pilot tunnel. This is also obvious from the observed small changes in normalized flow rate noticed in the field, cf. Chapter 7.

The above stated observations indicate that other plausible explanation for the observed discrepancy between measured and calculated parameters has to be addressed. One such is the presence of a skin zone of different permeability in the fracture in the immediate vicinity of, and circumpheral to the excavation. The results of the FRACT8E model suggests that the permeability skin ought to be positive (decreased permeability) along the walls and roof to reduce the calculated head drop and negative (increased permeability) in the floor to enhance the observed head drop somewhat in the F family of holes.

These changes are addressed in the subsequent model generation.

Table 6.1 Material properties of the areas around the pilot tunnel excavation where skin is assumed to have developed, cf. Figure 6.1.

	Permeability k (* 10^{-8} m^2)		
Area	FRACT8F:1	FRACT8F:2	FRACT8F:3
Slash	0.002	0.0002	0.0002
Floor A	0.50	0.50	0.50
Floor B	0.20	0.20	0.20
Floor C	-	-	0.002

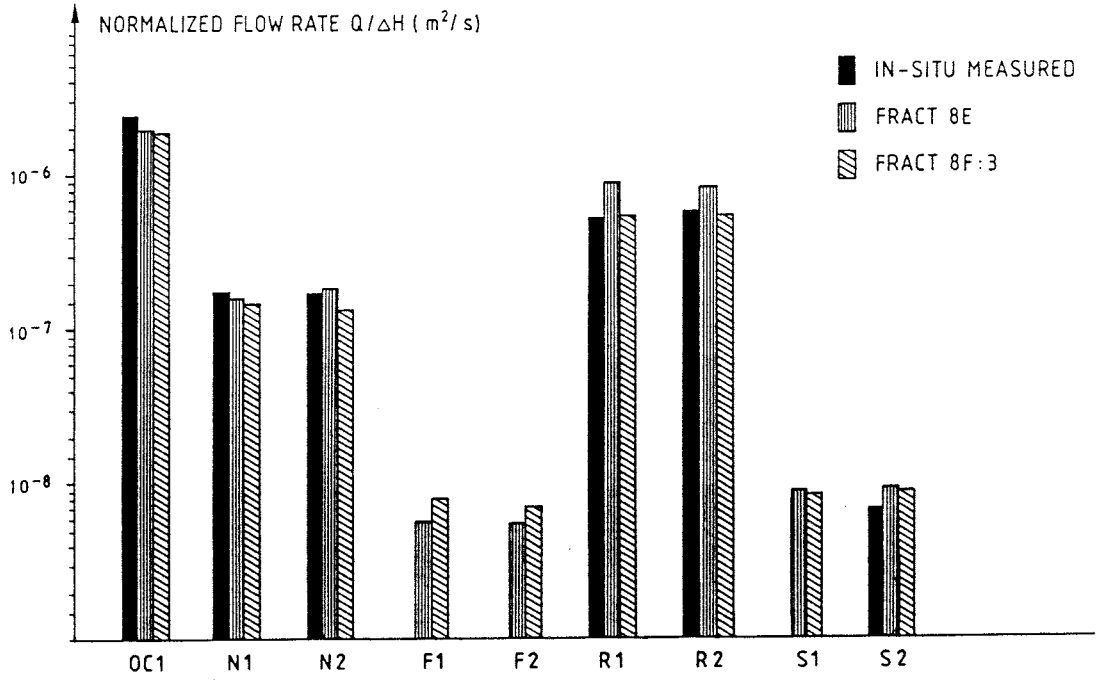

Figure 6.3 In-situ measured and calculated normalized flow rate in the tested boreholes for the case when the pilot tunnel is excavated.

6.3 Model generation V (FRACT8F)

6.3.1 General

Model generation V, FRACT8F, is made up of three different models, FRACT8F:1-3, all addressing the sensitivity in the model due to the presence of skin around the pilot tunnel. The areas where skin has been introduced are indicated in Figure 6.1. The skin zone along the south and north walls and the roof corresponds to the crossectional area of the subsequent slash round through the fracture (the actual thickness chosen is arbitrary and based on computational convenience). The skin or excavation damaged zone in the floor is described in four layers of elements forming three groups (A, B and C), cf. Figure 6.1.

The material properties of the models are identical to those of the FRACT8C model apart from the pilot crossection and the areas where skin is assumed to prevail. The material properties of the latter areas are listed in Table 6.1.

6.3.2 Simulation of head drop and inflow due to pilot tunnel

The steady state head drops have been calculated for the three sub-models. The results, cf. Table 6.2 and Figure 6.2, indicate that the head drops are aptly described for the FRACT8F:2 case. However, too much water is drawn from the northern part of the model causing a too high a drawdown in OC1 and the N pair of holes. By decreasing the permeability of the northern part of the floor, (area C) cf. Figure 6.1, a lower drawdown in the mentioned boreholes is obtained, as described in model FRACT8F:3.

Table 6.2 In-situ measured and calculated head drop due to the pilot intercept with the Room 209 fracture.

Borehole	Steady state head drop ΔH (metres)				
	In-situ*)	FRACT8E	FRACT8F:1	FRACT8F:2	FRACT8F:3
OC1	0.8	9.7	3.7	3.5	1.2
N1	4.0	38.4	26.0	25.7	7.7
N2	3.9	55.4	37.7	33.6	10.6
F1	104.0	86.4	99.0	99.5	97.8
F2	99.4	82.8	97.2	97.1	94.0
R1	2.5	64.1	3.3	2.0	0.7
R2	2.1	53.4	3.1	2.0	0.7
S1	10.7	57.6	25.6	12.2	11.4
S2	4.6	41.8	14.7	7.8	7.0

*) Values deduced from revised pressure drops compiled by B. Nakka (May 25 1988) based on data in Lang et al (1988c).

The resulting steady state inflow into the pilot tunnel as a consequence of the intercept of the fracture is compiled in Table 6.3. From the results it is obvious that the introduction of skin in the FRACT8F submodels shifts the distribution of flow entering the tunnel from the roof (FRACT8E) to the floor. FRACT8F:3 shows a deceivingly close correspondence with the measured quantity in terms of magnitude. However, the distribution of inflow does not compare well with the distribution of measured/estimated inflow compiled by Kozak in Lang et al (1988c), cf. Table 6.3. It should however be emphasized that the measurement/estimation of inflow through the floor was difficult and is subject to further studies (AECL 1988).

6.3.3 Simulation of single hole drawdown tests

Drawdown tests have only been simulated for model FRACT8F:3 which incorporates a fully developed skin and which best describes the head drop and total inflow to the pilot tunnel. The results expressed as normalized flow rates are presented in Table 6.4 and Figure 6.3 together with the corresponding results for the no skin case (FRACT8E) and the in-situ results.

The simulated normalized flow rates for the skin case (FRACT8F:3) are within 30% of the in-situ measured data. The R pair of holes show a good correspondence whereas S2 show an overestimation of 30%. The remaining comparable boreholes show underestimations within 30%.

In Table 6.5 a comparison is made how well the skin and no-skin models describe the relative change in normalized flow rate when the conditions are transitioned from pre-excavation state to a fully excavated pilot tunnel. The results are compared with the corresponding field results.

Table 6.3 Distribution of in-situ measured and calculated inflow to the pilot tunnel along the Room 209 fracture trace.

	Inflow to the pilot tunnel (litres/min)				
Portion of trace	In-situ	FRACT8E	FRACT8F:1	FRACT8F:2	FRACT8F:3
Roof	0.1	3.72	0.07	0.002	0.002
Floor	0.1*)	0.09	0.69	0.701	0.302
S wall	0.00	0.02	0.03	0.001	0.001
N wall	0.1*)	0.70	0.03	0.001	0.002
Sum total	0.3	4.5	0.8	0.7	0.3

*) The total contribution along the northernmost part of the floor and the north wall is estimated at 0.2 l/min (Kozak in Lang et al 1988c).

Table 6.4 Simulated and actual in-situ drawdown test results for the case when the pilot tunnel is excavated.

	Normalized flowrate (Q/ΔH) (* 10^{-9} m^2/s)		
Borehole	In-situ*)	FRACT8E	FRACT8F:3
OC1	2340.0	1950.0	1890.0
N1	173.0	160.0	147.0
N2	171.0	182.0	132.0
F1	-	5.7	8.2
F2	-	5.6	7.2
R1	528.0	892.0	540.0
R2	583.0	848.0	568.0
S1	-	9.0	8.6
S2	6.9	9.5	8.7

*) Average of nine tests following the intercept of the fracture by the pilot tunnel during the period Oct 27-Nov 19 1986), cf. Table 2.1.

Table 6.5 Relative change in normalized flow rate at the different borehole intercepts of the fracture due to transition from pre-excavation to post-pilot conditions.

Borehole	Q/ΔH (pre-)/Q/ΔH (post-)		
	In-situ*)	FRACT8E	FRACT8F:3
OC1	1.026	0.964	0.995
N1	0.971	0.906	0.986
N2	0.982	0.725	1.000
F1	-	0.880	0.607
F2	-	0.918	0.711
R1	1.439	0.633	1.041
R2	1.158	0.679	1.014
S1	-	1.009	1.063
S2	1.884	0.943	1.021

*) $Q/\Delta H$ (Oct 16 1986)/$(Q/\Delta H)_{mean}$ (Oct 27-Nov 13 1986)

When looking at the sign of the change in normalized flow rate (less or higher than unity) one finds that the skin case follows the observed pattern for the different boreholes though not in magnitude. The case with no skin (FRACT8E) shows an increase in transmissivity in all boreholes but one.

7. CONCLUSIONS

A post-analysis revision of an existing hydraulic model of the Room 209 fracture has been performed where all available information has been included. The model was calibrated against pre-excavation data and was subsequently used to analyse discrepancies between in-situ measured and calculated hydraulic responses to the introduction of a pilot tunnel.

The calculated hydraulic head distribution of the final pre-excavation model (FRACT8C) at points corresponding to the packed off sections in the Room 209 instrument array indicates that the in-situ head distribution is recreated within 5%, cf. Section 5.4.

The results of the simulated hydraulic testing (draw down tests) with the final pre-excavation model (FRACT8C) indicate that the in-situ testing results in terms of normalized flow rate ($Q/\Delta H$) have been described within 75%. The simulated interference tests, cf. Section 5.4.3, show at least a qualitative correspondence with in-situ results.

These findings indicate that the final pre-excavation model is a reasonable representation of the studied system in the steady state. It should however be emphasized that it is one out of many other possible ones.

It is also concluded that the assumed boundary conditions along the upper horizontal and northern vertical boundaries are reasonable.

The calculated response of a pilot tunnel excavation in the final calibrated pre-excavation model (FRACT8E, equivalent to model FRACT8C but with simulated pilot tunnel) indicates an overestimation of calculated head drops at the borehole locations within a factor 30 when compared with the in-situ measurements. The calculated inflow to the tunnel along the fracture trace is overestimated by more than one order of magnitude, the majority of the inflow emanating from the roof.

It was found that although flow out of roughly 50% the model element surfaces delineating the simulated boreholes was observed, the normalized flow rates obtained from simulation of drawdown tests in FRACT8E were overestimated. This suggests that the boreholes being subject to testing are positioned in a larger superimposed essentially radially converging flow field caused by the excavation itself.

It is considered that the change in normal stress in this particular case is unlikely to change the transmissivity of the Room 209 fracture drastically. This due to the small changes in normal stress noted (and calculated < 2 MPa) which are not high enough to appreciably alter the aperture of the fracture which has a very high normal stiffness (≈450 MPa/mm, Martin pers. comm.). This is also in line with the small changes in transmis-

sivity as inferred from single hole drawdown tests following the pilot excavation.

The noted underestimation (F1 and F2) and overestimation in head drops in the instrumented boreholes instead suggested the presence of skin zone of both increased permeability (negative skin) and decreased permeability (positive skin) in a thin (≈1 m) peripheral zone around the pilot excavation.

The skin model (FRACT8F:3) showed that the combined introduction of negative and positive skin could reproduce the in-situ head drops within a factor of 4. The calculated inflow to the tunnel in this case was very accurate although not entirely correct in terms of areal distribution.

It was also found that the skin model more accurately described the relative change in normalized flow rates in the single-hole drawdown tests as the excavation of the pilot tunnel was simulated.

The inferred positive skin may be due to propulsion of excavation debris into the fracture, causing clogging of the fracture close to the drift and/or temporary partial unsaturation of the corresponding parts of the fracture. The latter may be an agent causing the instantaneous drop in pressure and permeability observed upon pilot intercept followed by at least a partial resaturation, pressure build-up and increase in normalized flow rate, cf. Figure 2.3. The negative skin in the floor, on the other hand, is probably caused by the high energy explosive charges used in blast holes close to the floor and/or interconnection between the Room 209 fracture and excavation induced fractures in the floor.

It should however be emphasized that the physics of all these processes and their interaction are yet to be studied and analyzed more thoroughly.

The analysis shows that meaningful results explaining the noted discrepancies between measured and calculated hydraulic responses during the Room 209 Excavation Response Test may be obtained without necessarily using a coupled mechanical-hydraulic model. This has been achieved by lumping the possible occuring phenomena in the fracture into one single parameter, the skin.

8. RECOMMENDATIONS

8.1 General

This section is divided into two parts, the first focusing on recommendations applicable to the specific modelling exercise performed, and the second inclined towards a future Operating Phase ERE and experimental prerequisites with regard to perceivable future experiments in the Room 209 fracture, eg. a nuclide migration sorption experiment.

8.2 Modelling performed

A crucial assumption and simplification adopted in the modelling performed is that the fracture can be considered as a parallel plate. Even in-situ observations in the boreholes prior to excavation indicated that the Room 209 fracture is a zone of 1-6 fractures contained within a width of a few decimeters close to the tunnel. Additional information from boreholes to the north indicate a gradual increase in width with an interpreted thickness of some 5 m about 100 m north of Room 209.

Thus, one possible model alteration would be to test the model with 2D planar elements without adopting the parallel plate assumption, i.e. uncoupling the fracture aperture from the fracture permeability. This could be done for the model in its entirety or for subparts thereof, i.e. the near and far field.

In the cases where skin is described a possible scope for sensitivity analysis is to test the sensitivity in response to the radial extent of the assumed skin zone around the excavation. This could be accomplished without any severe changes in model geometry.

In the modelling performed, a hydraulic gradient in the far field of the fracture has been described based on observations in early 1988, cf. Section 3.4. The sensitivity in the assumed gradient, possibly addressing steeper gradients may be an other issue to address.

8.3 Production phase ERE and future experiments in the fracture

It is fully appreciated that the Room 209 Excavation Response Test was not initially intended to address also the hydraulic aspects of excavation response. In retrospect, the lack of data describing the far field contribute a great deal of speculation and forced inferences regarding these data. This applies both to the material property distribution and the boundary conditions of this part of the model.

The fact that the Room 209 fracture is a possible candidate for a single fracture migration and sorption experiment, probably at a larger scale than the tunnel area in the present model, calls for additional data related to the near and far field. The fact is that the part of URL covering the north extension of the Room 209 fracture, close to the shaft, is essentially uncharacterized by the URL surface borehole array.

With regard to a conceived future Operating Phase ERE it is probably most important to provide means to differentiate between possible responses induced by redistribution of stresses around the opening and that of the excavation method itself. Therefore a combination of excavation with explosives and tunnel boring techniques should be employed. It should however be emphasized that the rock debris produced by tunnel boring may be propelled into the fracture causing skin effects of the same type as

inferred in this study. Therefore careful consideration should be given to assess a mass balance of the debris theoretically produced.

Apart from the above effects, careful consideration should also be given to describe any desaturation/resaturation effects and possible impact on the hydraulics of fractures close to an underground opening due to changes in the climatological and chemical conditions.

As already pointed out by various researchers (eg. Simmons, pers. comm., Chan in Lang et al 1988b) in the post-excavation analysis, it is also of great interest to address the excavation response in a rock mass with a single or a multifold of fractures oriented parallel to the excavation axis. With that geometry, probably a higher magnitude of response would be encountered.

9. REFERENCES

AECL 1988 : Characterization of the 240 m Level of the Underground Research Laboratory. Progress report 1987 Oct-1988 March.

Chan, T., Griffiths, P.M. and Nakka, B. 1988 : Finite Element Modelling of Geomechanical and Hydrogeological Responses to the Room 209 Heading Extension Excavation Response Experiment : II. Post-excavation Analysis of Experimental results. Unpublished interim progress report.

Davison, C.C., Chan, T. and Scheier, N.W. 1987 : Experimental activities of the Canadian Nuclear Fuel Waste Management Program to Validate Geosphere Models, In Proc. of the GEOVAL Symp. 1987, vol. 2, pp. 401-422, Swedish Nuclear Power Inspectorate (SKI), April 7-9 1987.

Guvanasen, V. 1984 : Development of a Finite Element Hydrogeological Code and its Application to Geoscience Research. In Proceedings of 17th Information Meeting of the Nuclear Fuel Waste Management Program. Atomic Energy of Canada Limited Technical record TR-299.

Lang, P.A. 1988 : Room 209 Excavation Response Test in the Underground Research Laboratory, OECD/NEA Workshop on Excavation Response in Deep Radioactive Waste repositories, April 26-28, Winnipeg.

Lang, P.A., Everitt, R.A., Kozak, E.T. and Davison, C.C. 1988a : Underground Research Laboratory Room 209 Instrument array - Pre-excavation Information to Modellers. Atomic Energy of Canada Limited Report AECL-9566-1.

Lang, P.A. (ed) 1988b : Underground Research Laboratory Room 209 Instrument array - Modellers' Predictions of the Rock Mass Response to Excavation. Atomic Energy of Canada Limited Report AECL-9566-2.

Lang, P.A., Kuzyk, G.W., Babulic, P.J., Bilinsky, D.M., Everitt, R.A., Spinney, M.H., Kozak, E.T. and Davison, C.C. 1988c : Underground Research Laboratory Room 209 Instrument Array - Measured Response to Excavation. Atomic Energy of Canada Limited Report AECL-9566-3.

PDA Engineering 1985 : PATRAN user's guide. Santa Ana, CA, USA.

Simmons, G.R. 1988 : Geotechnical Research at Atomic Energy of Canada Limited's Underground Research Laboratory. Proc. of Canadian Nuclear Society Int. Symp. on Uranium and Electricity, Saskatoon, Saskatchewan, 1988 September 18-21.

Thompson, P.M., Kozak, E.T. and Martin, C.D. 1988 : Rock Displacement Instrumentation and Coupled Hydraulic Pressure/Rock Displacement Instrumentation for Use in stiff Crystalline rock. OECD/NEA Workshop on Excavation Response in Deep Radioactive Waste repositories, April 26-28, Winnipeg.

APPENDIX 1 Input material properties to models used to simulate the pre-excavation hydraulic conditions in the Room 209 fracture.

Model sub region	Permeability k (* 10^{-9} m^2)		
	FRACT8A	FRACT8B	FRACT8C
Far field	1.0000	1.0000	1.0000
Near field	2.1000	3.8300	3.8300
R1/R2 infl area	0.9400	0.9400	0.9400
N1/N2 infl area	0.3500	0.3500	0.3500
F1/F2 infl area	0.0340	0.0340	0.0284
S1/S2 infl area	0.0510	0.0510	0.0421
Granodiorite	0.0200	0.0200	0.0200

APPENDIX 2 Results of simulations of drawdown tests in boreholes in the Room 209 instrument array during pre-excavation conditions.

Borehole	Normalized flow rate $Q/\Delta H$ ($* 10^{-9}$ m^2/s)			
	In-situ	FRACT8A	FRACT8B	FRACT8C
OC1A	2400.0	890.0	1880.0	1880.0
N1	168.0	137.0	145.0	145.0
N2	168.0	125.0	132.0	132.0
F1	8.7	5.0	6.1	5.0
F2	2.2	6.2	6.4	5.1
R1	760.0	500.0	560.0	562.0
R2	675.0	405.0	576.0	576.0
S1	5.1	11.9	11.9	9.1
S2	13.0	11.7	11.7	8.9

List of SKB reports

Annual Reports

1977–78
TR 121
KBS Technical Reports 1 – 120.
Summaries. Stockholm, May 1979.

1979
TR 79–28
The KBS Annual Report 1979.
KBS Technical Reports 79-01 – 79-27.
Summaries. Stockholm, March 1980.

1980
TR 80–26
The KBS Annual Report 1980.
KBS Technical Reports 80-01 – 80-25.
Summaries. Stockholm, March 1981.

1981
TR 81–17
The KBS Annual Report 1981.
KBS Technical Reports 81-01 – 81-16.
Summaries. Stockholm, April 1982.

1982
TR 82–28
The KBS Annual Report 1982.
KBS Technical Reports 82-01 – 82-27.
Summaries. Stockholm, July 1983.

1983
TR 83–77
The KBS Annual Report 1983.
KBS Technical Reports 83-01 – 83-76
Summaries. Stockholm, June 1984.

1984
TR 85–01
Annual Research and Development Report 1984
Including Summaries of Technical Reports Issued during 1984. (Technical Reports 84-01– 84-19)
Stockholm June 1985.

1985
TR 85-20
Annual Research and Development Report 1985
Including Summaries of Technical Reports Issued during 1985. (Technical Reports 85-01-85-19)
Stockholm May 1986.

1986
TR 86-31
SKB Annual Report 1986
Including Summaries of Technical Reports Issued during 1986
Stockholm, May 1987

1987
TR 87-33
SKB Annual Report 1987
Including Summaries of Technical Reports Issued during 1987
Stockholm, May 1988

1988
TR 88-32
SKB Annual Report 1988
Including Summaries of Technical Reports Issued during 1988
Stockholm, May 1989

Technical Reports

1989
TR 89-01
Near-distance seismological monitoring of the Lansjärv neotectonic fault region Part II: 1988
Rutger Wahlström, Sven-Olof Linder,
Conny Holmqvist, Hans-Edy Mårtensson
Seismological Department, Uppsala University,
Uppsala
January 1989

TR 89-02
Description of background data in SKB database GEOTAB
Ebbe Eriksson, Stefan Sehlstedt
SGAB, Luleå
February 1989

TR 89-03
Characterization of the morphology, basement rock and tectonics in Sweden
Kennert Röshoff
August 1988

TR 89-04
SKB WP-Cave Project
Radionuclide release from the near-field in a WP-Cave repository
Maria Lindgren, Kristina Skagius
Kemakta Consultants Co, Stockholm
April 1989

TR 89-05
SKB WP-Cave Project
Transport of escaping radionuclides from the WP-Cave repository to the biosphere
Luis Moreno, Sue Arve, Ivars Neretnieks
Royal Institute of Technology, Stockholm
April 1989

TR 89-06
SKB WP-Cave Project
Individual radiation doses from nuclides contained in a WP-Cave repository for spent fuel
Sture Nordlinder, Ulla Bergström
Studsvik Nuclear, Studsvik
April 1989

TR 89-07
SKB WP-Cave Project
Some Notes on Technical Issues
Part 1: Temperature distribution in WP-Cave: when shafts are filled with sand/water mixtures
Stefan Björklund, Lennart Josefson
Division of Solid Mechanics, Chalmers University of Technology, Gothenburg, Sweden
Part 2: Gas and water transport from WP-Cave repository Luis Moreno, Ivars Neretnieks
Department of Chemical Engineering, Royal Institute of Technology, Stockholm, Sweden
Part 3: Transport of escaping nuclides from the WP-Cave repository to the biosphere. Influence of the hydraulic cage
Luis Moreno, Ivars Neretnieks
Department of Chemical Engineering, Royal Institute of Technology, Stockholm, Sweden
August 1989

TR 89-08
SKB WP-Cave Project
Thermally incuded convective motion in groundwater in the near field of the WP-Cave after filling and closure
Polydynamics Limited, Zürich
April 1989

TR 89-09
An evaluation of tracer tests performed at Studsvik
Luis Moreno[1], Ivars Neretnieks[1], Ove Landström[2]
[1] The Royal Institute of Technology, Department of Chemical Engineering, Stockholm
[2] Studsvik Nuclear, Nyköping
March 1989

TR 89-10
Copper produced from powder by HIP to encapsulate nuclear fuel elements
Lars B Ekbom, Sven Bogegård
Swedish National Defence Research Establishment
Materials department, Stockholm
February 1989

TR 89-11
Prediction of hydraulic conductivity and conductive fracture frequency by multivariate analysis of data from the Klipperås study site
Jan-Erik Andersson[1], Lennart Lindqvist[2]
[1] Swedish Geological Co, Uppsala
[2] EMX-system AB, Luleå
February 1988

TR 89-12
Hydraulic interference tests and tracer tests within the Brändan area, Finnsjön study site The Fracture Zone Project – Phase 3
Jan-Erik Andersson, Lennart Ekman, Erik Gustafsson, Rune Nordqvist, Sven Tirén
Swedish Geological Co, Division of Engineering Geology
June 1988

TR 89-13
Spent fuel
Dissolution and oxidation
An evaluation of literature data
Bernd Grambow
Hanh-Meitner-Institut, Berlin
March 1989

TR 89-14
The SKB spent fuel corrosion program Status report 1988
Lars O Werme[1], Roy S Forsyth[2]
[1] SKB, Stockholm
[2] Studsvik AB, Nyköping
May 1989

TR 89-15
Comparison between radar data and geophysical, geological and hydrological borehole parameters by multivariate analysis of data
Serje Carlsten, Lennart Lindqvist, Olle Olsson
Swedish Geological Company, Uppsala
March 1989

TR 89-16
Swedish Hard Rock Laboratory – Evaluation of 1988 year pre-investigations and description of the target area, the island of Äspö
Gunnar Gustafsson, Roy Stanfors, Peter Wikberg
June 1989

TR 89-17
Field instrumentation for hydrofracturing stress measurements
Documentation of the 1000 m hydrofracturing unit at Luleå University of Technology
Bjarni Bjarnason, Arne Torikka
August 1989

TR 89-18
Radar investigations at the Saltsjötunnel – predicitions and validation
Olle Olsson[1] and Kai Palmqvist[2]
[1] Abem AB, Uppsala, Sweden
[2] Bergab, Göteborg
June 1989

TR 89-19
Characterization of fracture zone 2, Finnsjön study-site
Editors: K. Ahlbom, J.A.T. Smellie, Swedish Geological Co, Uppsala
Part 1: Overview of the fracture zone project at Finnsjön, Sweden
K. Ahlbom and J.A.T. Smellie. Swedish Geological Company, Uppsala, Sweden.
Part 2: Geological setting and deformation history of a low angle fracture zone at Finnsjön, Sweden
Sven A. Tirén. Swedish Geological Company, Uppsala, Sweden.
Part 3: Hydraulic testing and modelling of a low-angle fracture zone at Finnsjön, Sweden
J-E. Andersson[1], L. Ekman[1], R. Nordqvist[1] and A. Winberg[2]
[1] Swedish Geological Company, Uppsala, Sweden
[2] Swedish Geological Company, Göteborg, Sweden
Part 4: Groundwater flow conditions in a low angle fracture zone at Finnsjön, Sweden
E. Gustafsson and P. Andersson. Swedish Geological Company, Uppsala, Sweden
Part 5: Hydrochemical investigations at Finnsjön, Sweden
J.A.T. Smellie[1] and P. Wikberg[2]
[1] Swedish Geological Company, Uppsala, Sweden
[2] Swedish Nuclear Fuel and Waste Management Company, Stockholm, Sweden
Part 6: Effects of gas-lift pumping on hydraulic borehole conditions at Finnsjön, Sweden
J-E- Andersson, P. Andersson and E. Gustafsson. Swedish Geological Company, Uppsala, Sweden
August 1989

TR 89-20
WP-Cave - Assessment of feasibility, safety and development potential
Swedish Nuclear Fuel and Waste Management Company, Stockholm, Sweden
September 1989

TR 89-21
Rock quality designation of the hydraulic properties in the near field of a final repository for spent nuclear fuel
Hans Carlsson[1], Leif Carlsson[1], Roland Pusch[2]
[1] Swedish Geological Co, SGAB, Gothenburg, Sweden
[2] Clay Technology AB, Lund, Sweden
June 1989

TR 89-22
Diffusion of Am, Pu, U, Np, Cs, I and Tc in compacted sand-bentonite mixture
Department of Nuclear Chemistry, Chalmers University of Technology, Gothenburg, Sweden
August 1989

TR 89-23
Deep ground water microbiology in Swedish granitic rock and it's relevance for radionuclide migration from a Swedish high level nuclear waste repository
Karsten Pedersen
University of Göteborg, Department of Marine microbiology, Gothenburg, Sweden
March 1989

TR 89-24
Some notes on diffusion of radionuclides through compacted clays
Trygve E Eriksen
Royal Institute of Technology, Department of Nuclear Chemistry, Stockholm, Sweden
May 1989

TR 89-25
Radionuclide sorption on crushed and intact granitic rock
Volume and surface effects
Trygve E Eriksen, Birgitta Locklund
Royal Institute of Technology, Department of Nuclear Chemistry, Stockholm, Sweden
May 1989

TR 89-26
Performance and safety analysis of WP-Cave concept
Kristina Skagius[1], Christer Svemar[2]
[1] Kemakta Konsult AB
[2] Swedish Nuclear Fuel and Waste Management Co
August 1989